Limnol. Oceanogr., 38(7), 1993, 1420–1437

Temporal variability of phytoplankton community structure based on pigment analysis

R. M. Letelier, R. R. Bidigare, D. V. Hebel, M. Ondrusek, C. D. Winn, and D. M. Karl

Department of Oceanography, School of Ocean and Earth Science and Technology, University of Hawaii, Honolulu 96822

Abstract

Algal chlorophyll and carotenoid distributions were measured periodically in the euphotic zone of Sta. ALOHA (22°45'N, 158°00'W) between February 1989 and October 1991 to document the variability in phytoplankton abundance and composition. The annual mean depth-integrated (0–200 db) concentration of Chl *a* displayed significant interannual variability. Seasonal patterns in Chl *a* concentration were found to be depth-dependent. Elevated Chl *a* in the mixed layer is the result of photoadaptation as the mixed layer deepens in winter. Increases in Chl *a* at the deep chlorophyll maximum layer (DCML) in spring are explained by increased nutrient availability caused by a deepening of the DCML relative to the $\sigma_\theta = 24.25$ density surface.

An algorithm based on the ratios of Chl *a* to diagnostic pigments present in specific algal taxa was used to estimate the contribution to total Chl *a* by the major algal groups represented within the DCML. Results indicate the presence of a phytoplankton community at the DCML with the following mean composition: *Prochlorococcus* spp. (39%), cyanobacteria (24%), prymnesiophytes (22%),and chrysophytes (13%). No single taxon is responsible for the springtime increase in Chl *a* observed in this habitat. Results from size fractionation and normal-phase high performance liquid chromatography confirm that *Prochlorococcus* spp. are the principal contributors of Chl *a* to the DCML.

The amplitude of the seasonal cycle in phytoplankton production and biomass is thought to be latitude-dependent with the smallest variations at low latitudes (Cushing 1959; Heinrich 1962; Sournia 1969). Consequently, mid- and low-latitude oceanic regions require robust sampling schedules and precise analyses to discern seasonal fluctuations in phytoplankton biomass and production from variability produced by stochastic events.

Acknowledgments

We are indebted to the HOT program scientists for assistance in the field, especially R. Lukas and his staff for the collection and analysis of the HOT program hydrographic data. We are grateful to J. Dore, S. Smith, J. Christian, R. Dawson, and an anonymous reviewer for criticisms and to L. Lum for help in preparing the manuscript. We thank the captains and crew of the RV *Moana Wave*, RV *Wecoma*, SSP *Kaimalino*, and RV *Alpha Helix* for assistance in the field.

The Hawaii Ocean Time-series (HOT) research program was supported, in part, by NSF grants OCE 88-00329 (D.M.K. and C.D.W.), OCE 90-16090 (D.M.K. and C.D.W.), OCE 87-17195 (R. Lukas), and BSR 90-18298 (R.R.B.), by State of Hawaii general funds and by a travel grant to R.M.L. by Fundacion Andes (Chile). NOAA provided support for SSP *Kaimalino* shiptime.

Contribution 3184 of the School of Ocean and Earth Science and Technology of the University of Hawaii.

The central North Pacific (CNP) gyre is considered to be a homogeneous, oligotrophic body of water located entirely in mid- and low-latitude regions (extending from ~15°N to 40°N and 135°E to 135°W). Several CNP gyre studies have addressed the mesoscale spatial variability of planktonic biomass (e.g. Hayward and McGowan 1985; Venrick 1979, 1990; Ondrusek et al. 1991). Temporal variability has also been reported at the "CLIMAX" area near 28°N, 155°W (Hayward et al. 1983; Hayward 1987) as well as near the Hawaiian Islands (Bienfang and Szyper 1981; Bienfang et al. 1984). However, seasonal variations in phytoplankton biomass remain poorly resolved or understood within this midocean habitat, even though they are an important aspect of community structure.

In the CNP gyre a permanent pycnocline in the lower portion of the euphotic zone restricts nutrient transport from the deep water to the upper 100 m of the water column (Eppley et al. 1973) and, consequently, limits the production of the region by limiting either its carrying capacity (Martin 1991) or the growth rate of its autotrophs (Thomas 1970; Falkowski et al. 1991). Under these conditions nutrient injections in the euphotic zone resulting from sporadic events such as wind-induced mixing

and dust deposition seem to be the principal cause of temporal variation in phytoplankton production and biomass (Platt and Harrison 1985; DiTullio and Laws 1991). Nevertheless, it is important to recognize that these events have a seasonal component. In the CNP gyre, sporadic injections of nutrients in the mixed layer as a result of storms or Asian dust depositions occur most frequently in winter and spring (DiTullio and Laws 1991; Donaghay et al. 1991; Young et al. 1991; Karl et al. 1992).

When investigating the temporal variability of phytoplankton biomass and processes in oligotrophic oceanic regions, it may be useful to uncouple fluctuations in the mixed layer from those occurring at the base of the euphotic zone. Injection of nutrients into the euphotic zone will primarily affect productivity above the deep chlorophyll maximum layer (DCML). On the other hand, increases in total solar irradiance measured at sea level from ~25 MJ $m^{-2} d^{-1}$ in autumn–winter to ~41 (Kirk 1983) in spring–summer may increase productivity of light-limited algal populations and alter community structure near the base of the euphotic zone. Thus, there are compelling reasons to expect that temporal variations in phytoplankton biomass and production are not uniform with respect to depth.

Since October 1988 the U.S.-Joint Global Ocean Flux Study (JGOFS) Hawaii Ocean Time-series (HOT) program has sponsored field studies at about monthly intervals at Sta. ALOHA (22°45′N, 158°00′W) to determine the temporal variability of physical and biogeochemical processes at a deep-water site representative of the CNP gyre (Karl and Winn 1991). Here we summarize algal chlorophyll and carotenoid distributions recorded during the first 3 yr of this program. We also analyze euphotic zone integrated (0–200 db) as well as depth-specific (mixed layer and DCML) temporal variability of Chl *a* concentration to look for evidence of a seasonal component. In addition we use accessory photosynthetic pigments as diagnostic markers of time-dependent changes in specific algal groups associated with the persistent DCML.

Materials and methods

Sample collection and preservation—Water samples for pigment analysis were collected as part of the core measurements performed at Sta. ALOHA (Fig. 1). A 24-position rosette water sampler equipped with 12-liter polyvinylchloride (PVC) bottles, SeaBird CTD, Beckman polarographic oxygen sensor, and a Sea Tech, Inc., flash fluorometer (ex, 425 nm; em, 625 nm) was used to sample the water column at predetermined depths. Samples (4–10 liters) from 8 to 14 reference depths (0–200 db) were collected between 2100–0600 hours and pressure filtered (N_2 at 27–55 kPa) through 25-mm-diameter glass-fiber filters (Whatman GF/F) under subdued lighting to protect the pigments from photooxidation. Eight of these depths were constant with respect to pressure throughout the study. The remaining depths were selected according to the continuous fluorescence trace generated in real time to increase sampling resolution near the DCML. The filters were flushed with N_2 gas and stored at −80°C until analyzed at our shore-based laboratories.

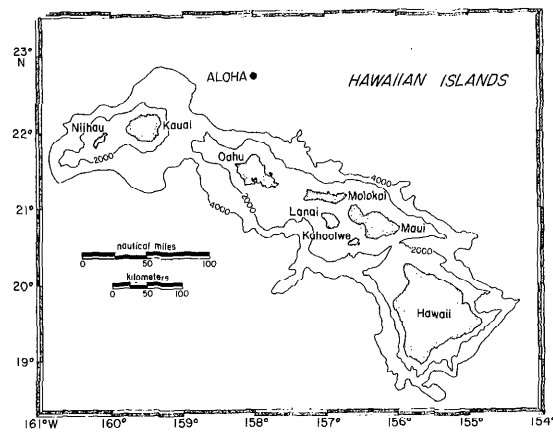

Fig. 1. Map showing the position of Sta. ALOHA. Contour lines are water depth in meters.

The reproducibility associated with sample collection and analysis was determined from duplicate sample bottles collected from the same depth during a single cast. Duplicate water samples collected on repetitive casts during a given cruise were used to determine small temporal and spatial scale (h-km) variability of pigment concentrations in the mixed layer and at the DCML.

CTD and fluorescence profiling—Short frequency cycles such as internal waves (minutes to hours), tides (12–25 h), and near-inertial period oscillation (31 h) may affect the vertical distribution of physical or biochemical param-

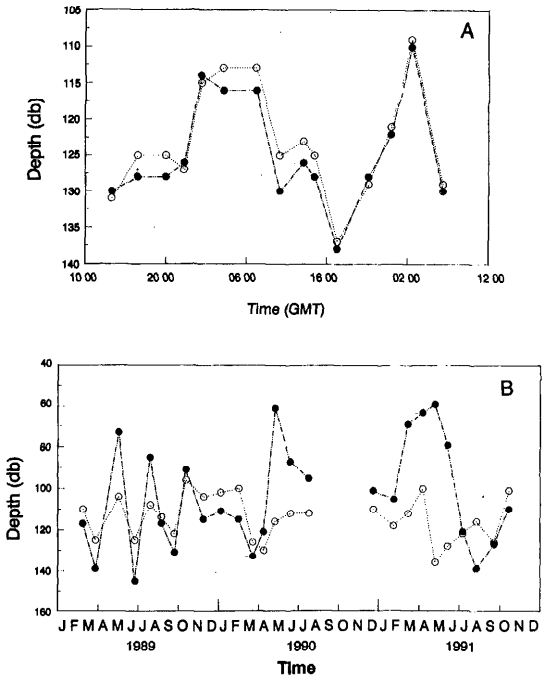

Fig. 2. Depth of the fluorescence maximum with respect to a reference isopycnal (σ_θ = 24.25) at Sta. ALOHA. A. Depth fluctuation over a 48-h period during HOT-30 (September 1991; local time, GMT + 10 h). B. Depth fluctuation, February 1989–October 1991. In this case the depths reported correspond to the average depth calculated for the 36-h observation period for each given cruise (*see text for details*). Symbols: ○—fluorescence maximum; ●—σ_θ = 24.25 density surface.

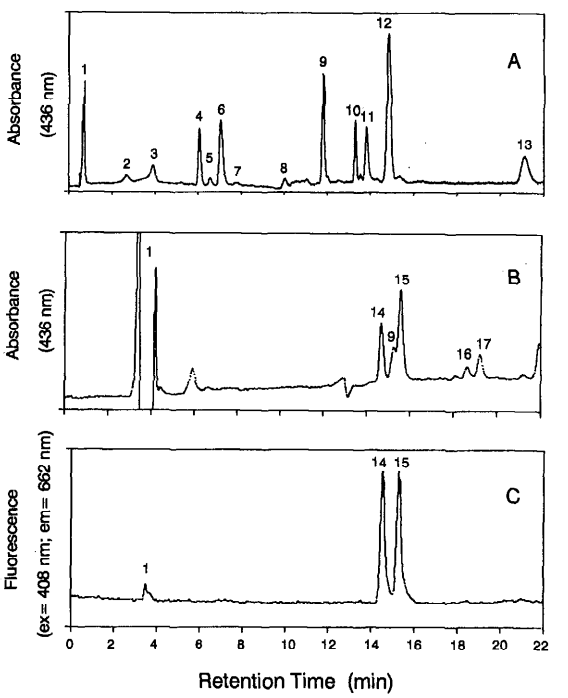

Fig. 3. Representative chromatograms. A. Absorption of reverse-phase separation of a 75-db sample (from HOT-31, October 1991). B. Absorption of normal-phase separation. C. Fluorescence of normal-phase separation. 1—Injection; 2—Chl c_3; 3—Chl c_1 + c_2 + Mg 3,8DVP a_5; 4—19′-but; 5—fucoxanthin; 6—19′-hex; 7—prasinoxanthin; 8—diadinoxanthin; 9—zeaxanthin; 10—Chl *b*; 11—canthaxanthin; 12—Chl *a*; 13—α-carotene; 14—Chl a_1; 15—Chl a_2; 16—Chl b_1; 17—Chl b_2.

eters at Sta. ALOHA by as much as 30 db in the euphotic zone. This variability was removed by adopting a 36-h burst sampling protocol (Karl and Winn 1991). CTD profiles (0–1,000 db) were taken at 3-h intervals for a 36-h period. During these repetitive casts, fluorescence profiles were also recorded as often as possible. The average depth of the physical parameters measured during the 36-h burst sampling period for each cruise is used here. Because the subsurface fluorescence maximum covaries with density rather than with depth on time scales of <48 h (Fig. 2A), the average depth of the DCML is defined by the average depth of the density surface corresponding to the fluorescence maximum for each cruise.

Pigment extraction and analysis—Pigments were extracted and analyzed by reverse-phase high performance liquid chromatography (HPLC) as described by Bidigare et al. (1989), with minor modifications. The frozen GF/F filters were placed into 3.1 ml of 100% acetone containing a known amount of canthaxanthin (also in acetone) as an internal standard. For each sample, 500 μl were injected automatically by a refrigerated (4°C) autosampler (Spectra-Physics model SP8880) into a Spectra-Physics model SP8800 HPLC equipped with a Radial-Pak C_{18} column (0.8 × 10 cm, 5-μm particle size, Waters Chromatogr.). Eluting peaks were detected by both absorbance (436 nm, Waters model 440 absorbance detector) and fluorescence (ex, 408 nm; em, 662 nm; Waters model 470 fluorescence detector) spectroscopy. Pigment concentrations were quantified by peak area with external standards provided as part of the JGOFS pigment intercalibration exercise. Routine identification of pigment peaks was based on retention time (Fig. 3A). In some instances, diode array spectroscopy (DAS; Waters model 990 pho-

Table 1. Ratios of diagnostic pigment markers for various algal groups used in the development of a taxonomic algorithm for attribution of measured Chl *a* into taxonomic compartments.

	Pigment ratio*	"Seed" value	Algorithm value	Source
Prochlorococcus spp.	$[\text{Chl } a]_{Prochl} = 0.91([\text{Chl}b] - 2.5[\text{prasino}]$			
	Chl *a* : Chl *b*	0.87	0.91	Goericke and Repeta 1992
	zeax: Chl *b*	0.29	0.07	
Cyanobacteria	$[\text{Chl } a]_{cyano} = 2.1\{[\text{zeax}] - 0.07([\text{Chl } b] - 2.5[\text{prasino}])\}$			
	Chl *a*: zeax	2.5	2.1	Kana et al. 1988
Chrysophytes	$[\text{Chl } a]_{chrys} = 0.9[19'\text{-but}]_{chrys}$			
	Chl *a* : 19′-but	3.82	0.9	Clone 1935-1 (CCMP 1145)
	fuco : 19′-but	1.39	0.14	
	19′-hex : 19′-but	0.14	0.14	
Prymnesiophytes	$[\text{Chl } a]_{prymn} = 1.3[19'\text{-hex}]_{prymn}$			
	Chl *a* : 19′-hex	1.6	1.3	*Emiliania huxleyi* (CCMP 373)
	fuco : 19′-hex	0.05	0.02	
	19′-hex : 19′-but	54.27	54.27	
Bacillariophytes	$[\text{Chl } a]_{bacill} = 0.8\{[\text{fuco}] - (0.02[19'\text{-hex}]_{prymn} + 0.14[19'\text{-but}]_{chrys})\}$			
	Chl *a* : fuco	0.8	0.8	*Phaeodactylum tricornutum* (CCMP 1327)
Dinoflagellates	$[\text{Chl } a]_{dino} = 1.5[\text{perid}]$			
	Chl *a* : perid	1.55	1.5	*Amphidinium* sp.
Prasinophytes	$[\text{Chl } a]_{pras} = 2.1[\text{prasino}]$			
	Chl *a* : prasino	2.54	2.1	*Pycnococcus provasolii* (CCMP 1203)
	Chl *b* : prasino	2.62	2.5	

* Abbreviations include prasinoxanthin (prasino), zeaxanthin (zeax), 19′-butanoyloxyfucoxanthin (19′-but), 19′-hexanoyloxyfucoxanthin (19′-hex), fucoxanthin (fuco), and peridinin (perid).

todiode array detector, 400–750 nm) was used to identify the unknown peaks and the dominant pigment in cases of co-elution [i.e. lutein + zeaxanthin and Chl c_1 + Chl c_2 + Mg 3,8divinyl-pheoporphyrin a_5 (Mg 3,8DVP a_5) peaks].

Three sets of pooled samples from below 45 db (>240 liters) collected between February 1989 and July 1990 and two sets of pooled samples from above 45 db (>180 liters) collected during the same period were used to determine the presence of lutein. From these samples, several visible absorption spectra were obtained during the lutein + zeaxanthin peak elution interval. The absence of a shift in the absorption maxima corresponding to zeaxanthin between the onset and the tail of the peak was taken as evidence for the absence of lutein in the sample.

The reverse-phase HPLC method used cannot separate monovinyl Chl *a* (Chl a_1) from divinyl Chl *a* (Chl a_2) or monovinyl Chl *b* (Chl b_1) from divinyl Chl *b* (Chl b_2), and thus provides estimates of total "Chl *a*" (Chl *a*) and "Chl *b*" (Chl *b*) concentrations, respectively. Chl a_2 and b_2 are the major chlorophyll forms found in *Prochlorococcus marinus* (Goericke and Repeta 1992) and can be separated from their monovinyl counterparts by normal-phase HPLC (Gieskes et al. pers. comm.). This separation was performed in size-fractionated samples (*see below*).

Estimation of the contribution of Chl a *by different algal groups*—Ratios of Chl *a* to accessory pigments characteristic of each group were obtained from previous studies and from the analysis of pigments extracted from phytoplankton cultures (Table 1). Because these ratios were determined for shade-adapted cultures, only samples collected between the 75- and 150-db reference depth strata were used in this analysis. These ratios (i.e. seed values) were further refined by inverse methods, determining the least-squares best solution to the equation $A \cdot \bar{x} = \bar{c}$, where A is a matrix of the accessory pigment concentrations, $\bar{x} = x_1, \ldots, x_n$ are the ratios of accessory pigments to Chl *a*, and $\bar{c} = c_1, \ldots, c_n$ are the measured Chl *a* concentrations (Tarantola 1987). Constraints were placed on the ratios of zeaxanthin : Chl *b* in *Prochlorococcus* spp., fucoxanthin (fuco): 19′-hexanoyloxyfucoxanthin (19′-hex) in prymnesiophytes, and fuco : 19′-butanoyloxyfucoxanthin (19′-but) in chrysophytes to avoid

solutions containing negative contributions of Chl *a* by a given algal taxon.

Prymnesiophytes and chrysophytes found in oceanic waters have similar major pigment signatures. We made two assumptions to assess the contribution of each taxon to the total Chl *a* based on the pigment algorithm: 19′-hex and 19′-but are found exclusively in these two algal groups, and the ratio between these two pigments in a given taxon remains constant at depths ≥75 db. Stauber and Jeffrey (1988) reported the presence of 19′-but in one diatom species and 19′-hex has been found in certain dinoflagellates (Tangen and Björnland 1981). However, because neither diatoms nor dinoflagellates are common in our study region, the first assumption appears to be valid. The second assumption remains untested.

The different amounts of 19′-hex and 19′-but contained in prymnesiophytes (prymn) and chrysophytes (chrys) were calculated by solving the following equations for each sample:

$$[19'\text{-hex}]_{\text{prymn}} = [P/(P - C)][(h_T - b_T C)]$$

and

$$[19'\text{-but}]_{\text{chrys}} = [P/(P - C)][b_T - (h_T/P)]$$

where h_T and b_T are the total concentrations of 19′-hex and 19′-but found in a given sample and P and C the 19′-hex : 19′-but ratios found in cultures of prymnesiophytes and chrysophytes ($P = 54.27$ and $C = 0.14$; Table 1).

DCML size-fractionation experiment—During the August 1991 cruise (HOT-29), five large-volume samples (12 liters each) collected near the DCML were filtered sequentially through 47-mm-diameter Poretics nylon membrane filters with porosities of 5, 1.2, 0.65, and 0.22 μm to determine the size-dependent variations in accessory pigment composition and to test the validity of the Chl *a* contribution algorithm. After extraction in 100% acetone and addition of the internal standard (canthaxanthin), all five samples for a given size fraction were combined and two 500-μl subsamples were removed from each size fraction for reverse-phase HPLC analysis, as described above.

The remaining extract of each size fraction was analyzed by normal-phase chromatography (Gieskes et al. pers. comm.). For this, pigments were quantitatively transferred to diethyl ether by adding diethyl ether to the acetone extract and shaking with cold 10% NaCl solution (volumetric ratio of acetone extract to diethyl ether to 10% NaCl solution = 3 : 3 : 30; cf. Barrett and Jeffrey 1971). To produce a full partitioning between the diethyl ether and aqueous phases, we added NaCl crystals to the emulsion. The diethyl ether phase was removed by Pasteur pipette and subsequently concentrated under N_2 in preparation for normal-phase HPLC analysis. The two solvent systems used consist of light petroleum ether (60–80°C), acetone, and dimethyl sulfoxide (DMSO) in the following proportions (by volume): A = 29 : 70 : 1 and B = 84 : 15 : 1. After injection (100 μl of concentrated diethyl ether extract), the linear elution gradient was developed over 20 min, starting with 100% A and ending with 40% of solvent A. Separations were performed on a 0.46 × 25-cm Spherisorb silica column (5-μm particle size) at a constant flow rate of 1 ml min^{-1}. A nearly complete baseline separation of Chl a_1, a_2, b_1, and b_2 was achieved with the procedure described above (Fig. 3B). Eluting peaks were detected in series with a Waters model 440 absorbance detector (435-nm filter; band width, 11 nm) and Waters model 470 fluorescence detector (ex, 408 nm; em, 662 nm).

Because the wavelength-dependent absorption properties of Chl a_1 and a_2 as well as Chl b_1 and b_2 in the Soret band region differ significantly, concentrations of Chl a_1, a_2, b_1, and b_2 were "spectrally corrected" to account for differences in the optical properties of these chlorophylls. In applying this spectral correction we have assumed that the weight-specific extinction coefficients (in the normal- and reverse-phase eluants) at the Soret absorption maxima of Chl a_1 and a_2 and Chl b_1 and b_2 are identical. On-line absorption spectra (400–500 nm) of the chlorophylls were measured during reverse-phase (Chl a_1 and b_1) and normal-phase (Chl a_1, a_2, b_1, and b_2) runs using a Waters model 990 photodiode array detector. The absorption properties of Chl a_2 and b_2 for reverse-phase conditions were estimated by red-shifting the Chl a_1 and b_1 spectra by 8 nm.

Absorption response weighting factors were individually computed by multiplying the absorption properties of each chlorophyll by the transmission characteristics of the 436-nm filter used for peak detection and then integrating with respect to wavelength. Under normal-phase conditions, the ratio of the calculated

Chl a_1 : Chl a_2 response factors was 0.714 and that of the calculated Chl b_1 : Chl b_2 response factors was 1.134. Under reverse-phase conditions the ratio of the calculated Chl a_1 : Chl a_2 response factors was 0.865 and that of the calculated Chl b_1 : Chl b_2 response factors was 1.377. The implication of these ratios is that, for environments where divinyl forms of chlorophylls are dominant, the 436-nm absorbance measured during reverse-phase HPLC runs may overestimate Chl *a* by 16% and underestimate Chl *b* by as much as 27%.

Because of a co-elution problem with Chl a_2 and zeaxanthin (Fig. 3B), Chl a_1 and a_2 were routinely detected by fluorescence spectroscopy (Fig. 3C). Normal-phase HPLC analysis of samples and prochlorophyte cultures which contained only minor amounts of zeaxanthin (i.e. Chl a_2 and zeaxanthin were baseline separated) allowed establishment of a linear relationship between the absorbance and fluorescence peak areas measured (in series) for Chl a_1 ($r^2 = 0.98$, $n = 7$) and Chl a_2 ($r^2 = 0.97$, $n = 6$). Thus, for a routine normal-phase HPLC run, fluorescence peak areas were used to compute absorbance peak areas for these chlorophylls and eliminate the zeaxanthin co-elution problem. For Chl b_1 and b_2, directly measured absorbance peak areas were used in the following computations.

The peak areas measured for Chl a_2 and b_2 under normal-phase conditions were multiplied by factors of 0.714 and 1.134, respectively, to correct for differences in the absorption properties of these chlorophylls relative to their monovinyl counterparts (*see above*). After these corrections were applied, spectrally corrected ratios of Chl a_1 : (Chl a_1 + Chl a_2) and Chl b_1 : (Chl b_1 + Chl b_2) were computed for each sample. These ratios were used in conjunction with the reverse-phase absorption correction factors presented above to partition the total "Chl *a*" and "Chl *b*" concentrations (i.e. determined by reverse-phase HPLC) into absolute concentrations of Chl a_1, a_2, b_1, and b_2.

Ancillary HOT program data—Core measurements of hydrography, suspended particulate matter and dissolved nutrients, and measurement protocols for the HOT program that were obtained in conjunction with the pigment data presented herein are available via the worldwide Internet system and anonymous file transfer protocol (ftp). The data are in a subdirectory called /pub/hot. The workstation's Internet address is iniki.soest.hawaii.edu.

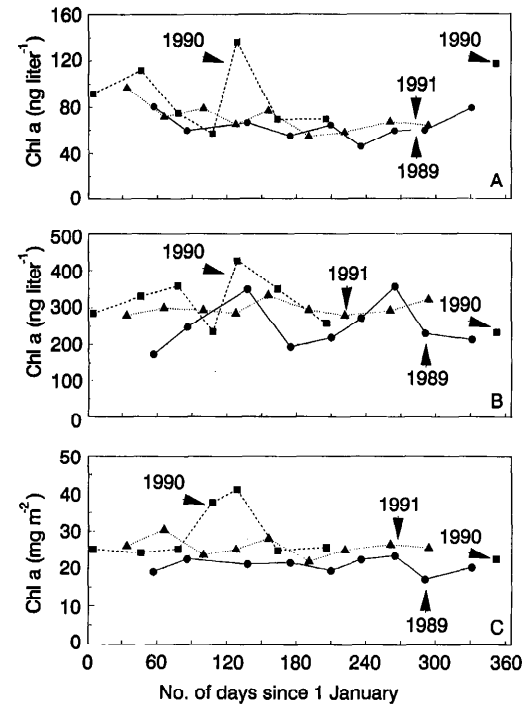

Fig. 4. Temporal variability of Chl *a*. A. Concentrations of Chl *a* at 5-m depth. B. DCML Chl *a* concentrations. C. Chl *a* concentrations integrated from 0- to 200-db depth.

Results

Variability in mixed-layer and DCML depth—During the 3-yr period of this study, the surface mixed-layer depth (defined here as a density gradient ≤ 0.005 σ_θ units db^{-1}) varied between 15 and 120 db. The mean depth of the DCML, based on the continuous fluorescence traces, was 112 db with boundary values at 96 and 136 db (Fig. 2B). Our 36-h burst sampling procedures revealed an even broader range in the DCML depth (70–150 db) due to effects which we interpret as internal waves. Although the potential density associated with the DCML remained constant for a given cruise (Fig. 2A), σ_θ values from the entire data set ranged from 23.77 to 24.94, indicating vertical displacement of the DCML across isopycnal surfaces throughout the 3-yr period of observations.

Integrated and depth-specific Chl a variability—Euphotic zone depth-integrated (0–200 m)

Table 2. Chlorophyll and major accessory pigment concentrations measured for various reference depths, February 1989–October 1991.

Pigment	5 m (ng liter $^{-1}$)		DCML (ng liter $^{-1}$)		0–200-m depth integrated (mg m $^{-2}$)	
	Mean*	Range	Mean*	Range	Mean*	Range
Chl *a*	78±21	46–137	282±59	173–427	24.5±6.2	17.2–41.2
Chl *b*	†		123±44	45–188	8.6±2.2	4.7–14.6
Chl $c_1 + c_2$	4±3	2–12	32±28	16–56	3.0±2.2	1.4–8.9
Chl c_3	3±2	2–6	16±8	8–41	1.6±0.9	0.6–4.7
Peridinin‡	—		—		—	
19′-but	5±2	2–9	40±14	15–66	3.4±1.0	2.3–6.0
Fucoxanthin	7±3	2–13	8±4	4–17	1.1±0.5	0.4–2.2
19′-hex	10±2	6–13	54±17	34–92	4.3±1.0	2.9–6.5
Prasinoxanthin§	—		—		—	
Diadinoxanthin	5±1	3–8	6±2	2–11	0.8±0.2	0.4–1.2
Zeaxanthin	50±10	29–69	43±15	24–87	6.4±1.4	4.4–10.2

* ±1 SD.
† Sporadically detected with values ranging from <0.2 to 12 ng liter $^{-1}$.
‡ Sporadically detected with values ranging from <0.1 to 3 ng liter $^{-1}$ for 5 m, from <0.2 to 6 ng liter $^{-1}$ for the DCML, and from <0.7 to 6 mg m $^{-2}$ for 0–200 m.
§ Sporadically detected with values ranging from <0.1 to 2 ng liter $^{-1}$ for 5 m, from <0.2 to 6 ng liter $^{-1}$ for the DCML, and from <0.6 to 4 mg m $^{-2}$ for 0–200 m.

values of Chl *a* determined by reverse-phase HPLC analysis varied from 17.2 to >40 mg m^{-2} ($\bar{x}$ = 24.5 mg m^{-2}, s = 6.2; Fig. 4C). Mixed-layer concentrations of Chl *a*, measured at the 5-db reference depth, ranged from 46 to 137 ng liter^{-1} ($\bar{x}$ = 78 ng liter^{-1}, s = 21; Fig. 4A); values in the DCML varied from 173 to 427 ng liter^{-1} ($\bar{x}$ = 282 ng liter^{-1}, s = 59; Fig. 4B). Replicate casts taken in May 1989, June 1989, and July 1991 indicated that the reproducibility of major pigment concentration measurements at these two layers was within 15% for a given cruise.

Over the period of this study, euphotic zone depth-integrated Chl *a*, as well as mixed-layer and DCML Chl *a* concentrations showed similar variability (C.V. = 25, 27, and 21%). There was no significant correlation between mixed layer and euphotic zone depth-integrated Chl *a* concentrations (r^2 = 0.14, n = 26, $P > 0.05$). A significant interannual variability was found in euphotic zone depth-integrated Chl *a*. During 1989 the mean concentration ($\bar{x}$ = 20.9 mg m^{-2}, s = 2.0; n = 9) was significantly lower ($P < 0.05$) than in 1990 or 1991 ($\bar{x}$ = 28.4 mg m^{-2}, s = 7.0; n = 8 and $\bar{x}$ = 25.9 mg m^{-2}, s = 2.4; n = 9; Fig. 4C). Also, although the annual average concentration of Chl *a* at the DCML did not vary significantly between 1989, 1990, and 1991 (250, 310, and 298 ng liter^{-1}), the C.V. ranged from 24.27% in 1989 to 5.8% in 1991.

Distribution of accessory photosynthetic pigments—The most abundant accessory pigments detected were Chl *b*, zeaxanthin, 19′-hex, 19′-but, Chl *c*, and fucoxanthin. Trace concentrations of diadinoxanthin were also detected during every cruise. Prasinoxanthin was detectable only in late winter and spring, and peridinin was present only sporadically (Table 2). Pheopigments were a minor component in the water column during all cruises. Other than Chl *b*, pigment markers of chlorophytes (violaxanthin and lutein) were consistently below the level of detection (<0.5 ng liter^{-1} for violaxanthin and no shift of absorption maxima corresponding to zeaxanthin during the elution of the lutein + zeaxanthin peak for lutein) in all samples analyzed, even though fairly large volumes of water were processed (4–10 liters per sample).

Vertical profiles of pigments at Sta. ALOHA displayed a characteristic DCML oscillating around the 0.5% isolume (mean depth of 112 db). The "light depth" of this layer, however, varied between the 3% and the 0.08% isolumes (70 and 150 db) as a result of vertical displacements of the density field and fluctuations of depth-specific absolute photosynthetically available radiation (PAR) caused by changes in the intensity of sea-surface light.

Zeaxanthin was the dominant accessory pigment in the mixed layer, and although its concentration declined with depth, a secondary peak was generally detected at the DCML. Chl *b*, 19′-hex, and 19′-but concentrations were low in surface waters but increased with depth to maximum concentrations near the DCML;

Chl *b* was the most abundant accessory pigment at the DCML (Figs. 5 and 6). Prasinoxanthin profiles had an irregular pattern, with maximum concentrations located between 75 and 125 db (Fig. 6).

Chl a *taxonomic algorithm*—Chl *a* concentrations predicted from the taxonomic algorithm are in excellent agreement with Chl *a* concentrations measured in both the individual and depth-integrated (75–150 db) samples. Profiles comparing both predicted and measured Chl *a* values for samples collected in October 1991 and not used for the generation of the algorithm also show excellent agreement for depths ≥50 db (Fig. 6). The predicted values, however, deviate from measured concentrations above 50 db (data not shown).

On the basis of our photosynthetic pigment model, four algal groups contribute >95% of the total Chl *a* measured at the DCML: *Prochlorococcus* spp. (39%), cyanobacteria (24%), prymnesiophytes (22%), and chrysophytes (13%) (Fig. 7). For depth-integrated (75–150 db) Chl *a*, the respective contributions are 35, 31, 20, and 10%. Other minor (<1%) contributors to total Chl *a* were prasinophytes, dinoflagellates, and diatoms. Chlorophytes, if present at all, comprised a negligible fraction of the total Chl *a*.

A highly significant positive correlation was found for the Chl *a* contributed by *Prochlorococcus* spp. and chrysophytes (Kendall rank correlation $P < 0.001$). No significant correlation was found between Chl *a* contributed by these groups and Chl *a* contributed by cyanobacteria ($P > 0.1$). Nevertheless, all groups but dinoflagellates were positively correlated with measured Chl *a* concentrations ($P < 0.02$).

Size distribution and algal accessory pigments—In our samples 19′-hex dominated the >5-μm fraction while smaller fractions were dominated by Chl b_2 (Table 3). The sum of all size fractions reveals that for the DCML in August 1991, 70% of Chl *a* and 77% of Chl *b* were in the divinyl form (i.e. Chl a_2 and b_2; Table 3). Only the fraction >5 μm was dominated by Chl a_1 and 75% of Chl b_1 was retained by a 1.2-μm pore-size filter. Most other accessory pigments were present only in traces for size fractions <1.2 μm where zeaxanthin and Chl b_2 are the dominant accessory pigments. Peridinin and diadinoxanthin were in notably low concentrations at the DCML during this cruise (Table 3).

Table 3. Pigment distribution in different size fractions from water collected near the DCML, August 1991.

	Particle size class (μm)			
	>5	5–1.2	1.2–0.65	0.65–0.22
	Concentration (ng liter^{-1})			
Peridinin	1	*	*	*
19′-but	13	16	3	0.2
Fucoxanthin	3	2	*	*
19′-hex	28	11	2	0.2
Diadinoxanthin	2	1	*	*
Zeaxanthin	6	7	12	6
Chl *b*				
monovinyl	15.4	7.7	7.2	0.7
divinyl	15.7	24.7	53.9	9.9
Chl *a*				
monovinyl	54.9	8.0	8.5	1.8
divinyl	28.2	55.5	65.9	21.3
Chl $a_{\text{algorithm}}$	83.4	63.5	76.7	21.1

* Below detection limit, which for these assay conditions were peridinin (0.05 ng liter^{-1}), fucoxanthin (0.04 ng liter^{-1}), and diadinoxanthin (0.02 ng liter^{-1}), assuming equal distribution of pigments in each size fraction.

These size fractionation data also allowed a further test of the taxonomic contribution model for different size classes. In general, there was very good agreement between measured Chl *a* and that predicted by the model (Table 3). Particles >5 μm were mainly prymnesiophytes, *Prochlorococcus* spp., chrysophytes, and cyanobacteria (41, 33, 13, and 10% of the total Chl *a*). Although 100% of the diatom and dinoflagellate diagnostic pigments were restricted to the largest size fraction, these taxa accounted for <3% of the total Chl *a*.

Discussion

Interannual variability in Chl a *concentrations*—As reported previously by Hayward and Venrick (1982) and Hayward (1987), euphotic zone values of depth-integrated Chl *a* appear to vary in time by a factor of < 3. Nevertheless, the mean annual concentration calculated for 1989 is significantly lower than those calculated for 1990 and 1991. The first year also exhibited a high variability in Chl *a* concentrations at the DCML when compared to subsequent years. Relatively strong displacement of isopycnal surfaces in the euphotic zone during 1989 (Fig. 5A) and the consequent frequent migrations of the DCML through these surfaces (Fig. 2B) may have perturbed the phytoplankton community in this layer, resulting in low concentrations of Chl *a*.

Based on the analysis of samples collected in summer (May–October), Venrick et al.

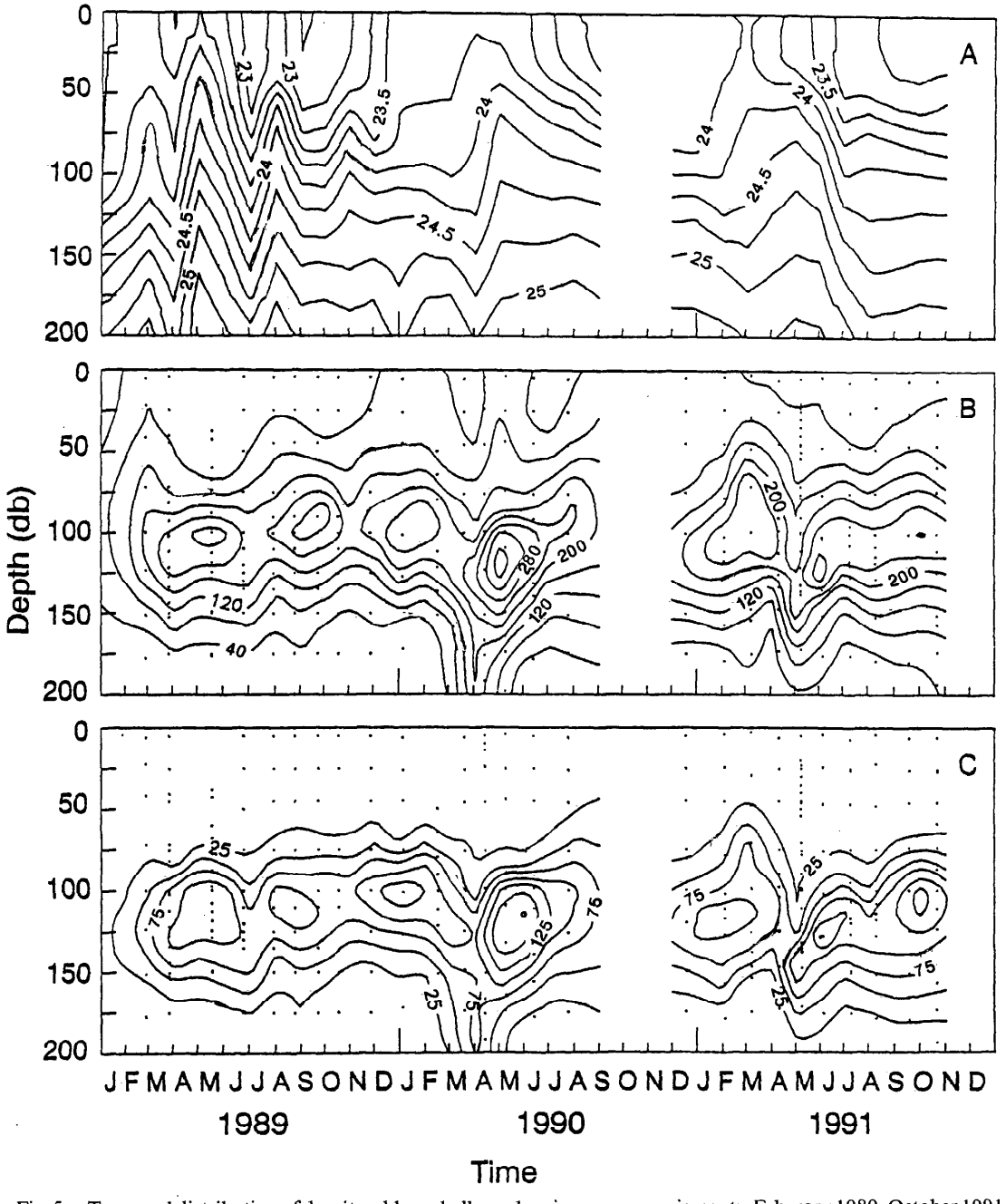

Fig. 5. Temporal distribution of density, chlorophylls, and major accessory pigments, February 1989–October 1991. A. Density (σ_θ). B. Chl *a* (ng liter^{-1}). C. Chl *b* (ng liter^{-1}). D. Zeaxanthin (ng liter^{-1}). E. 19′-hex (ng liter^{-1}). F. 19′-but (ng litcr^{-1}).

(1987) presented evidence for a significant increase of euphotic zone depth-integrated Chl *a* in the CNP gyre between 1964 and 1985. Although our values of euphotic zone depth-integrated Chl *a* are not rigorously comparable with theirs (i.e. use of Whatman GF/F instead of GF/C filters and HPLC instead of fluorometric quantification), the combination of both

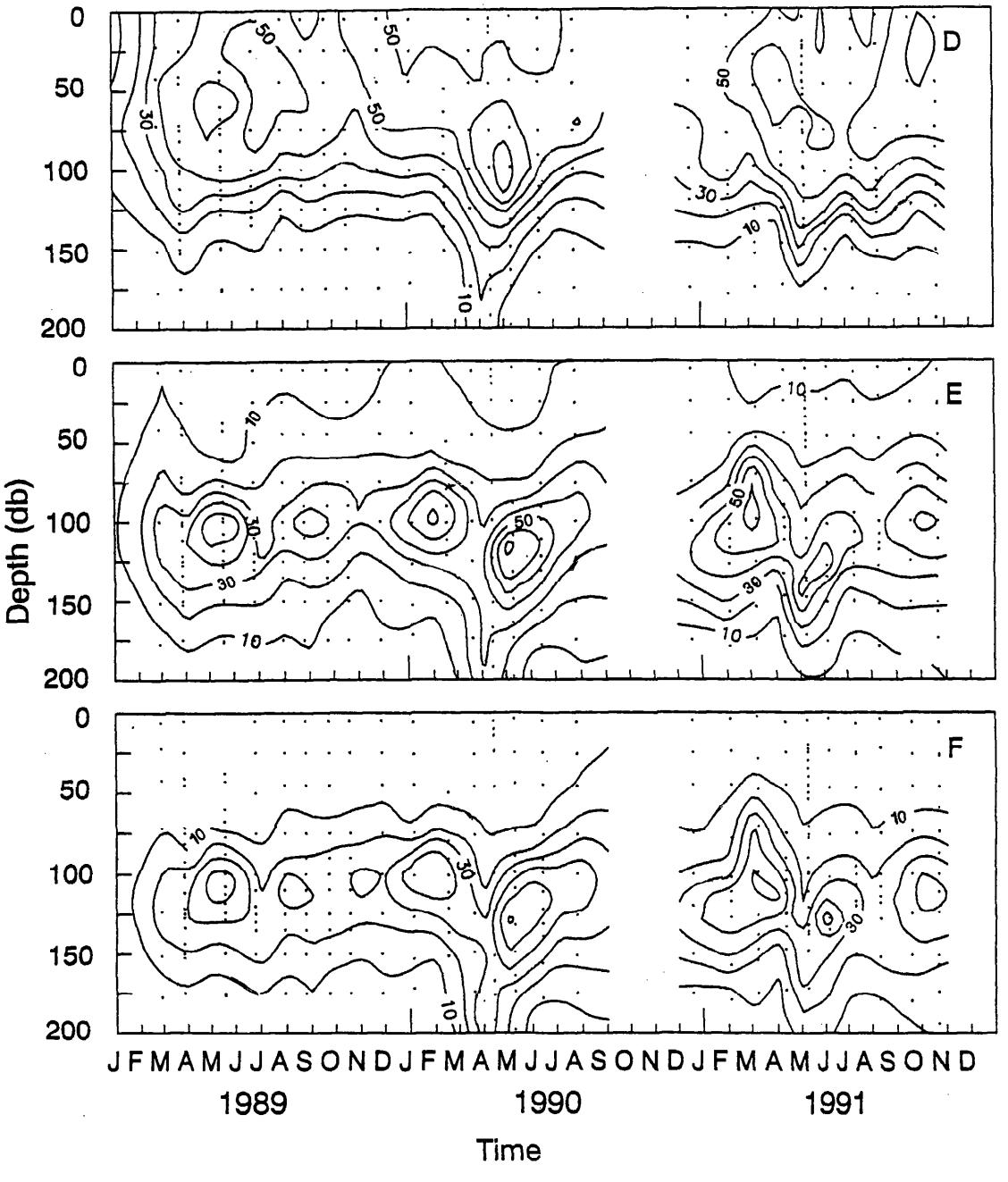

Fig. 5. Continued.

data sets suggests that since 1980 concentrations of Chl *a* have remained high in comparison to values reported prior to 1974. Nevertheless, it is important to note a significant ($P < 0.05$) interannual variability of summer (May–October) mean Chl *a* concentration between 1989 (20.9 mg m^{-2}) and the following years ($\bar{x}$ = 30.7 and 25.9 mg m^{-2} for 1990 and

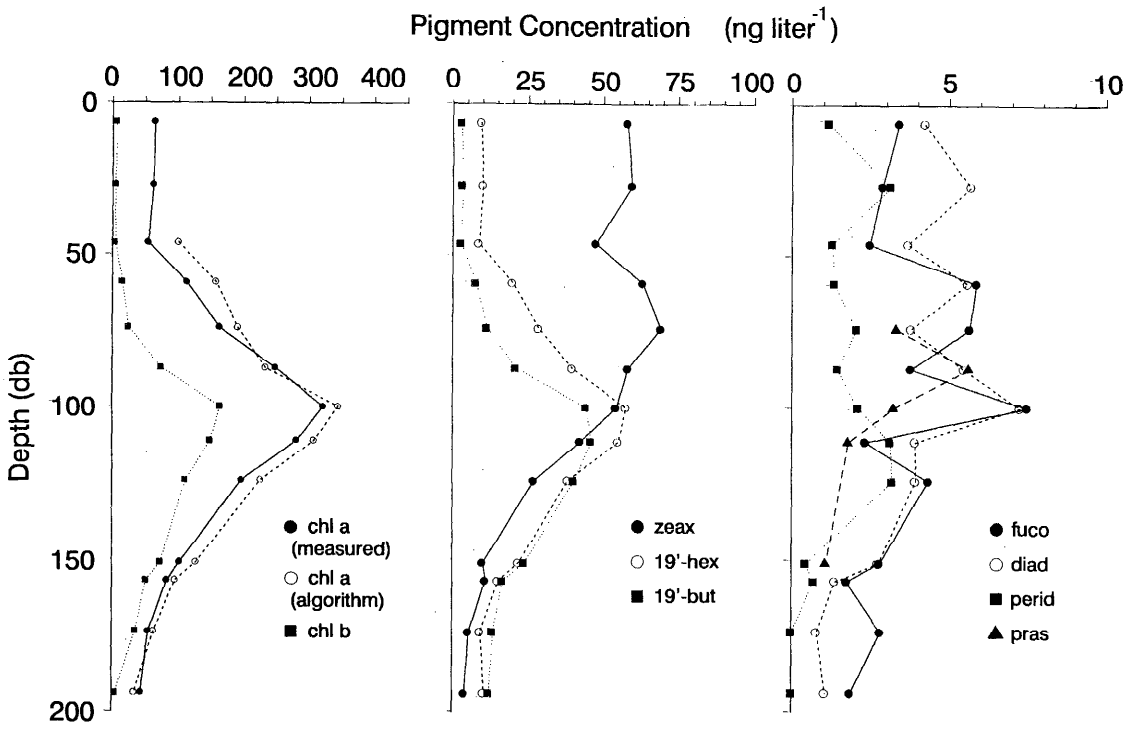

Fig. 6. Profile concentrations of chlorophylls, major accessory pigments, and Chl *a* predicted by the taxonomic model during HOT-31 (October 1991).

1991). The range of this variability is almost as large as the range observed by Venrick et al. (1987) between Chl *a* measurements made before 1974 and after 1980.

Mixed-layer intra-annual variability—Mixed-layer concentrations of Chl *a* exhibit maxima (>80 ng liter^{-1}) commonly associated with winter months. Only concentrations <70 ng liter^{-1} and usually lower than the annual mean concentration are found during summer in the mixed layer (Figs. 4A and 8A). One exception to this pattern is the high concentration of Chl *a* measured in June 1990. A strong upward displacement of isopycnals (Figs. 2B and 5A) and a significant increase of net production over the upper 75 m of the euphotic zone (Winn et al. 1991) suggests the sampling of a cyclonic eddy core during that cruise.

High concentrations of Chl *a* near the surface in winter are associated with wind-induced deep (>80 db) mixed layers (Chiswell et al. 1990; Winn et al. 1991, 1993). Two processes may account for a rise in Chl *a* concentrations under these conditions. The first is an increase of phytoplankton standing stock due to the input of inorganic nutrients. This input may occur either as a flux of nutrients from the base of the mixed layer if it reaches the depth corresponding to the top of the nutricline (~110–120 m) or as a flux to the sea surface from the combined effects of wet and dry deposition (DiTullio and Laws 1991; Young et al. 1991). The data collected at Sta. ALOHA are inconclusive as to the influence of either of these mechanisms to account for an increase in near-surface Chl *a* concentration. Increases in Chl *a* do not correlate with increases in particulate C (PC), particulate N (PN), or particulate adenosine triphosphate (P-ATP) concentrations during winter mixing events. Neither is there any direct evidence of increased inorganic nutrient pools in the euphotic zone, even though the HOT program routinely uses analytical methods designed to measure N and P at nanomolar levels (Winn et al. 1993).

Phytoplankton photoadaptation due to deepening of the mixed layer is also considered to be an important factor responsible for the increase of Chl *a* in surface layers (Ohman et

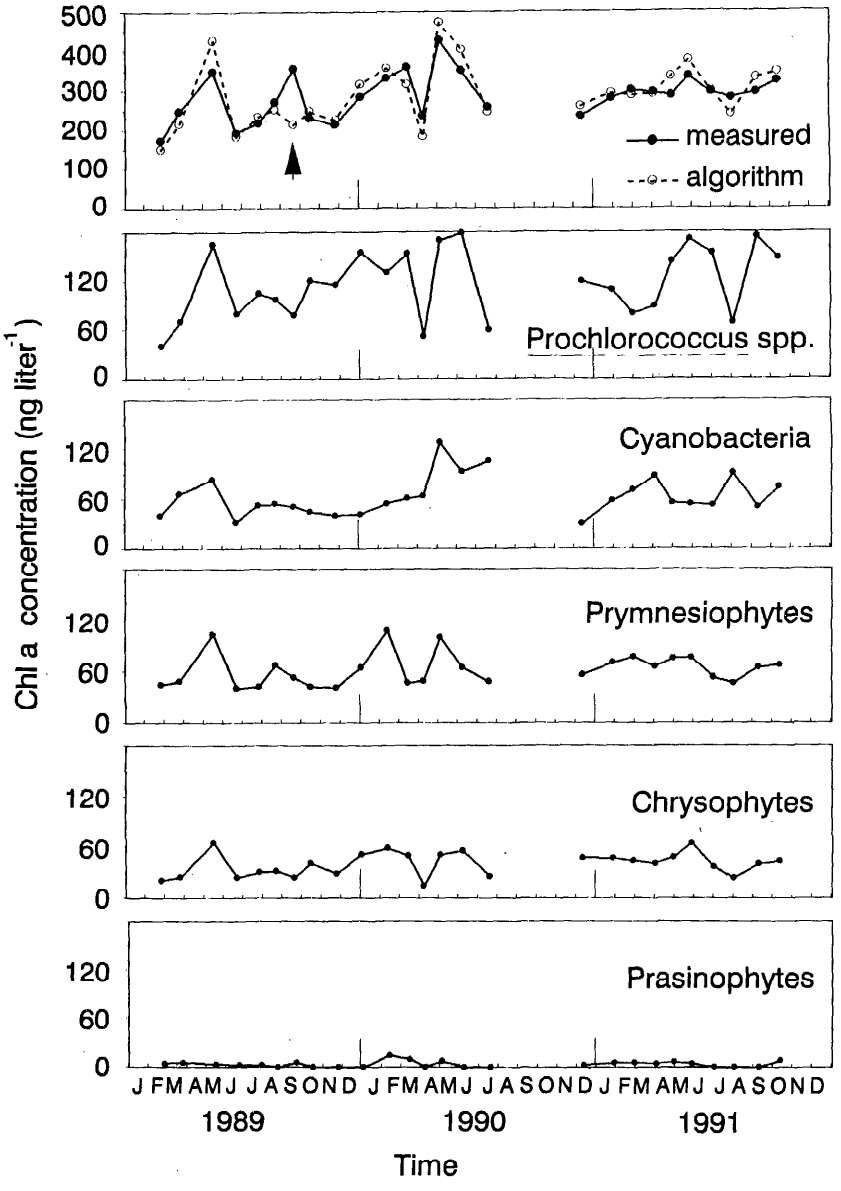

Fig. 7. Comparison of Chl *a* measured and accounted for by the taxonomic algorithm and calculated contributions of the major algal groups to the total Chl *a* in the DCML. Arrowhead shows the deviation of the predicted Chl *a* from the concentration measured during HOT-10 (September 1989).

al. 1982). During wintertime deep mixing events, the ratio of phytoplankton C (calculated as P-ATP × 250 × 0.7; Karl 1980; Laws et al. 1984) to Chl *a* decreases from an average of 91 to values ranging from 31 to 63. In contrast, summer values may be as high as 133 (Chiswell et al. 1990; Winn et al. 1991, 1993). Although the absolute magnitude of this ratio is not indicative of photoadaptation per se (Banse 1977), the relatively low values observed during winter mixing may reflect an increase in light-harvesting complexes due to a decline in the average mixed-layer light (Shuter 1979; Laws et al. 1983). The enhancement in Chl *b* and *c* and the decrease in photoprotective pigment concentrations (zeaxanthin and

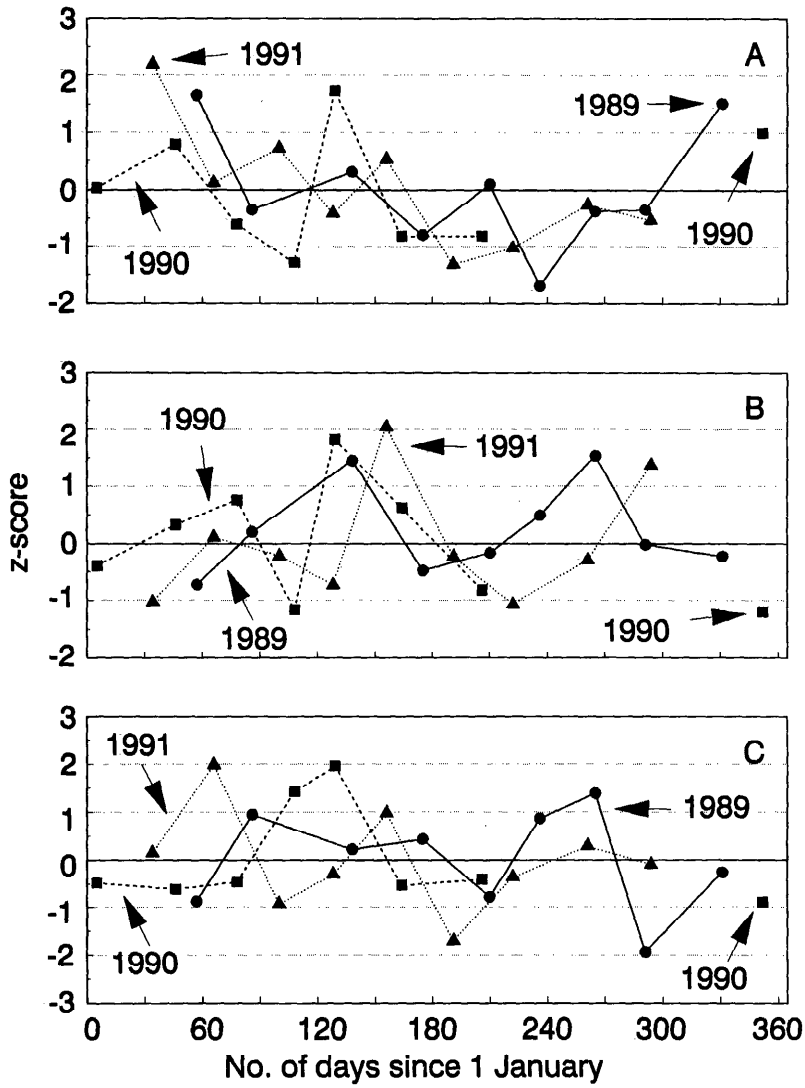

Fig. 8. Z-score [$z = (x - \bar{x})s^{-1}$; where x is the measured value, $\bar{x}$ is the annual mean for that calendar year, and s is 1 SD of the annual mean for that year] of Chl *a* concentration, February 1989–October 1991: A—5 m; B—DCML; C—integrated from 0- to 200-m depth.

diadinoxanthin) give further support to photoadaptation as a causal mechanism for the increase of Chl *a* during winter mixing events.

DCML intra-annual variability—In contrast to the pattern observed in the near-surface layer, Chl *a* concentrations in the DCML show evidence of an increase in spring (Fig. 7). This feature is clearly observed when the standard *z*-score (Triola 1989) of each value based on annual means and variances [$z = (x - \bar{x}_y)s_y^{-1}$, where y represents the year during which x was measured] is calculated (Fig. 8B). A strong positive deviation from the annual mean appears during spring of each of the three consecutive years thus far studied. A positive deviation is also suggested for autumn of the 2 yr where data are available. For 1989 and 1990 the strongest positive cross-correlation is found when the lag period is nil ($r = 0.69$); for 1991, it appears with a 30-d lag period with respect to 1989 or 1990 ($r = 0.77$ and $r = 0.66$).

During the first 2 yr, the increases of DCML Chl *a* concentrations observed in spring coincide with an increase in PC and PN at 100

m; in 1991 PC and PN values rise 1 month before the Chl *a* maximum was measured at the DCML. In theory, an increase in the depth of light penetration may provide enough radiant energy to nutrient-sufficient phytoplankton to result in a transient accumulation of biomass or an accumulation of cells via active migration at the DCML. This change in the underwater light field would translate not only into enhancement of the biomass, but also into deepening of the DCML in spring. The average depth of the fluorescence maximum calculated for each cruise deepens during March–May and, although the DCML depth seems to covary with vertical movements of the $\sigma_\theta = 22.45$ isopycnal, the covariance is at a minimum in spring (*see 1990 and 1991 in Fig. 2B*). Maximum concentrations of Chl *a* at the DCML have been measured not in association with the deepest fluorescence maximum but during the following month when the DCML is below the $\sigma_\theta = 24.6$ isopycnal.

McGowan and Hayward (1978) and Venrick (1990) proposed that the breaking of internal waves or the upward displacement of isopycnal surfaces could play an important role in the input of nutrients into the euphotic zone. In our study, inorganic nutrient concentrations at the fluorescence maximum layer do not show a correlation with Chl *a* concentrations at this depth (Chiswell et al. 1990; Winn et al. 1991, 1993). This finding is to be expected given our sampling frequency and the potential for rapid nutrient uptake by phytoplankton. However, nutrient samples collected at Sta. ALOHA are not filtered before the analyses of total dissolved N (TDN) and total dissolved P (TDP), so theoretically we should be able to assess nutrient injections into the base of the euphotic zone unless there is a simultaneous and coupled particulate export to the mesopelagic zone. To the contrary, our data suggest a decrease in TDN and TDP concentrations at the DCML during spring Chl *a* events (Chiswell et al. 1990; Winn et al. 1991, 1993).

If high concentrations of Chl *a* and accessory pigments at the DCML represent increases in algal biomass, as suggested by the increase in PC and PN (Chiswell et al. 1990; Winn et al. 1991, 1993), the apparent loss in the TN and TP pools can be reconciled only by an increase in particle export. However, the increase in algal biomass in our study indicates a lag time between the increase in primary production and the increase in grazing on the order of days to weeks.

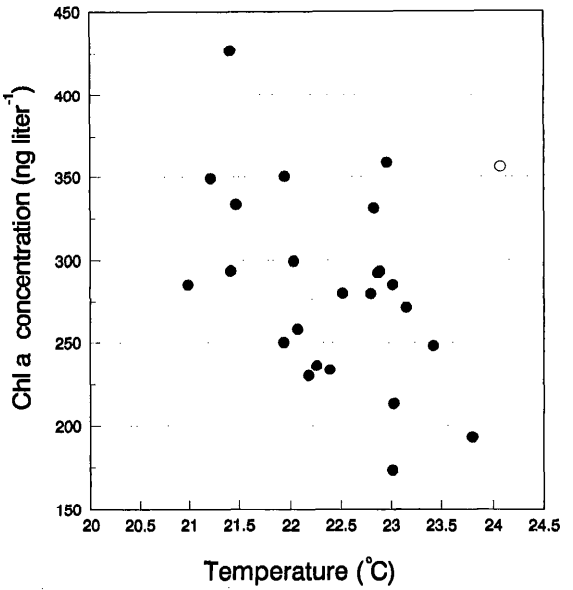

Fig. 9. Chl *a* concentrations measured at the DCML plotted against the measured temperature at 100 db for each cruise, February 1989–October 1991. Data from HOT-10 (September 1989—O) have been excluded from this analysis.

If we assume that temperature is a more stable and conservative indicator of deep-water intrusions into the euphotic zone than nutrient concentrations, we should expect an inverse relationship between temperature and Chl *a* concentrations in the lower euphotic zone. When plotting average temperature at 100 m vs. Chl *a* concentration in the DCML (Fig. 9), we find that high concentrations are generally present during cooler periods, while values <250 ng liter^{-1} are restricted to temperatures >22°C. One clear exception to this trend is found for September 1989. This increase relative to the expected value based on temperature may have been caused by an input of nutrients mediated by a bloom of the nitrogen-fixing cyanobacterium *Trichodesmium* spp. observed the previous month at Sta. ALOHA. *Trichodesmium* spp. blooms have been considered an important alternative source of new nitrogen (Carpenter and Romans 1991; Karl et al. 1992) and of other limiting nutrients (Devassy et al. 1978, 1979) in oligotrophic oceans.

Our results suggest that increases of Chl *a* in the DCML at Sta. ALOHA in spring are due to the deepening of this layer relative to isopycnals. These deepenings are the result of an increase in the daily average irradiance combined with the intrusion of nutrient-rich waters into the euphotic zone due to the upward vertical displacement of isopycnal surfaces. Although there is no clear explanation for this apparently seasonal vertical displacement of the pycnocline, possible mechanisms may involve changes in the energy of eddy fields or Rossby waves affecting the flow east of the Hawaiian Ridge or a decrease in the transfer of heat from the sea surface to depth as a result of an increase in stratification of the water column in spring and summer.

Accessory pigment composition and the taxonomic algorithm—The general pigment composition of phytoplankton at Sta. ALOHA is similar to the one reported by Ondrusek et al. (1991) for the CNP gyre. The absence of detectable concentrations of violaxanthin and lutein suggests that chlorophytes are relatively rare in the water column at this location. Although our HPLC method does not separate lutein from zeaxanthin, the lack of a shift in the absorption maxima corresponding to zeaxanthin during the peak elution indicates that $<10\%$ of the absorption recorded for this peak is due to lutein. The presence of high Chl b_2: Chl b_1 in all samples analyzed by normal-phase HPLC throughout the water column during this study (data not shown) supports the conclusion that chlorophytes are a negligible component of the phytoplankton assemblage in these waters. Chl b_1 may be attributed to prasinophytes when present. The absence of detectable amounts of violaxanthin further suggests that chrysophytes found at Sta. ALOHA correspond to "aberrant" chrysophytes as described by Withers et al. (1981), Vesk and Jeffrey (1987), and Bidigare (1989).

The taxonomic model presented here accounts for most of the temporal and vertical variability of Chl *a* below the mixed layer ($>93\%$). However, because the principal factors affecting the ratios of Chl *a* to accessory pigment are light intensity and spectral quality and because both vary with depth, some caution must be applied in interpreting the vertical distribution of our taxonomic analyses. By restricting our study to the portion of the water column between 75 and 150 db, the error associated with the assumption of constant pigment ratios with depth is minimized. Furthermore, it is important to emphasize that, during the period of study, the "light depth" of the DCML remained between the 3% and 0.08% isolumes where Chl *a*: accessory pigment ratios should be close to constant for a given taxonomic group. Consequently, we feel that the temporal analysis of pigments in this layer and the derived community structure are probably indicative of real temporal changes in phytoplankton processes at the DCML.

Also, because this algorithm was developed for the phytoplankton assemblage found at Sta. ALOHA, it may be invalid for communities found in other marine environments. This may explain some of the large discrepancies between "seed values" and ratios used in the final algorithm. Nevertheless, sensitivity analyses reveal that the use of unaltered seed values for the Chl *b*: zeaxanthin ratio in *Prochlorococcus* spp. and 19′-but: fuco ratio in chrysophytes results in negative contributions of Chl *a* by cyanobacteria and bacillariophytes, respectively.

By decomposing the measured Chl *a* near the DCML into different algal class contributions, we observe that the spring increases in Chl *a* are the result of an increase in all of the major algal groups, with the exception of cyanobacteria in 1991, rather than any single component (Fig. 7). Nevertheless, the relative contribution to Chl *a* by each algal class does not remain constant during these events. Although prymnesiophytes and chrysophytes present small fluctuations in their relative contributions over time, the proportions of Chl *a* attributed to *Prochlorococcus* spp. and cyanobacteria have larger fluctuations and are negatively correlated (Kendall rank correction, $P < 0.01$). A strong positive correlation is found between variations in the Chl *a* concentration attributed to *Prochlorococcus* spp. and Chl *a* concentration attributed to chrysophytes ($P < 0.001$), while Chl *a* concentration attributed to cyanobacteria is not correlated with the above groups ($P > 0.2$). Prymnesiophytes, on the other hand, are positively correlated with all major taxa.

These correlations suggest the presence of at least two algal associations at the DCML. When normalized to Chl *a* concentrations, Chl *b* and

19′-but always increase with depth in the vicinity of the DCML (112±15 db). Neither zeaxanthin nor 19′-hex ratios show any pattern at this depth. From these characteristic pigment signatures, we infer that *Prochlorococcus* spp. cells and chrysophytes are better adapted for existence at the base of the DCML. Similar patterns of pigment concentrations close to the base of the euphotic zone have been reported for the Atlantic Ocean (Gieskes and Kraay 1986; Bidigare et al. 1990).

Vertical displacements of the DCML due to movements of the water column or changes in sea surface light intensity (Banse 1987) result in high variability of the daily radiant energy available to phytoplankton at the DCML. Because most phytoplankton groups found in the DCML are not active migrators and light intensity is considered to be close to limiting values at this depth stratum, PAR variability may have a major influence on the composition of the phytoplankton community, maintaining a dynamic equilibrium between these algal associations. In this case, internal waves and other inertial oscillations of isopycnals around the DCML (Fig. 2A) may have a greater influence on phytoplankton rate processes than seasonal effects in this layer and may contribute significantly to maintenance of taxonomic diversity. However, because algal biomass is controlled by nutrient availability and net growth rate, the fluctuation in total Chl *a* is more likely to reflect changes in one or both of these parameters than changes in the phytoplankton community structure. This conclusion is supported by the significant correlation ($P \leq 0.02$) observed between the contribution to Chl *a* of all algal groups (with the exception of dinoflagellates) and total Chl *a* measured at the DCML.

Size fractionation of DCML samples—Because different phytoplankton taxa have different size spectra, the size fractionation results allow a rigorous test of the taxonomic algorithm. In general there is excellent agreement between Chl *a* measured and Chl *a* accounted for by the algorithm in the different size fractions (Chl a_{alg} = 1.005 Chl a_{meas}; $r^2 = 0.996$, $n = 4$). As expected, dinoflagellates and bacillariophytes are restricted to the largest size fraction (>5 μm), accounting for <3% of the Chl *a* in that fraction. *Prochlorococcus* spp. and cyanobacteria dominate the <5- to >0.22-μm fraction, accounting for 58 and 14% of the total Chl *a* in this size range. However, it should be emphasized that the distribution of Chl *a*, taken as an indirect estimate of biomass, may not reflect a priori the actual role of the various taxonomic groups in biogeochemical cycles; metabolic rates may be uncoupled from pigment and biomass distributions.

The large proportion of Chl *a* attributed to *Prochlorococcus* spp. in the >5-μm size fraction (33.4%) may be the result of cells associated with marine snow particles retained by the filter. This proportion does not differ from the fraction of Chl *a* found as Chl a_2 (33.9%) in the same size fraction. Cyanobacteria in this size fraction could be *Synechococcus* spp. cells also associated with marine snow as well as filaments of *Trichodesmium* spp. trapped by the filter. Flow cytometric analysis of replicate 1-ml samples collected before and after the filtration of 10 liters of DCML seawater through a 5-μm Poretics nylon membrane filter indicates that there is no significant retention of "free" *Prochlorococcus* cells (as determined by the combined light scatter and fluorescence signatures) during the filtration procedure ($t = 0.833$; df = 10; $P < 0.05$).

Finally, although the taxonomic algorithm seems to account for all the Chl *a* measured in samples collected around the DCML, discrepancies are found when comparing the fraction of Chl *a* attributed to *Prochlorococcus* spp. by using the algorithm and the percentage of Chl *a* found in divinyl form (Chl a_2) in the size fractions 5–1.2 μm and 0.65–0.22 μm (Table 3). These discrepancies may be the result of Chl *b* erroneously attributed to *Prochlorococcus* spp.

Although pigment markers of chlorophytes or prasinophytes other than Chl b_1 are not detected in our size-fractionated samples, we cannot rule out the possibility that these pigments are present in concentrations below the limit of detection. A chlorophyte clone isolated recently from Sta. ALOHA by L. Campbell has a Chl b_1 : violaxanthin ratio of 10.3. Because the limit of detection for violaxanthin in our study is 0.1 ng liter^{-1}, we would only be able to detect violaxanthin if chlorophytes contributed at least 1.0 ng Chl b_1 liter^{-1} in a given size fraction, assuming that the isolated clone is representative of all chlorophytes at Sta. ALOHA. A similar calculation can be per-

formed to calculate the potential contribution to Chl b_1 by prasinophytes with pigment ratios from Table 1.

Recently, Partensky et al. (1993) reported that two clones of *Prochlorococcus* isolated from the North Atlantic (SARG and NATL1) produce Chl b_1 when kept under blue growth irradiances (5 and 13% of the total Chl *b*). Their report suggests the possibility that *Prochlorococcus* spp. are major contributors of the Chl b_1 measured during our DCML size fractionation study.

The discrepancies between the fraction of Chl *a* attributed to *Prochlorococcus* spp. by using the algorithm and the percentage of Chl *a* found as Chl a_2 may also be caused by size-dependent differences in accessory pigment: Chl *a* ratios within a given algal group. From our data it is apparent that the ratio of Chl a_2 to Chl b_2 for *Prochlorococcus* spp. is not constant across different size fractions. We hypothesize the coexistence of at least two physiologically diverse populations of *Prochlorococcus* with distinct pigment signatures and size spectra in the DCML at Sta. ALOHA. More detailed studies combining algal pigment quantification with flow cytometric analyses in size-fractionated samples will help test this hypothesis.

References

BANSE, K. 1977. Determining the carbon-to-chlorophyll ratio of natural phytoplankton. Mar. Biol. **41:** 199–212.

———. 1987. Clouds, deep chlorophyll maximum, and the nutrient supply to the mixed layer of stratified water bodies. J. Plankton Res. **9:** 1031–1036.

BARRETT, J., AND S. W. JEFFREY. 1971. A note in the occurrence of chlorophyllase in marine algae. J. Exp. Mar. Biol. Ecol. **7:** 255–262.

BIDIGARE, R. R. 1989. Photosynthetic pigment composition of the brown tide alga: Unique chlorophyll and carotenoid derivatives, p. 57–75. *In* E. Cosper et al. [eds.], Novel phytoplankton blooms. Springer.

———, AND OTHERS. 1990. Evidence for phytoplankton succession and chromatic adaptation in the Sargasso Sea during spring 1985. Mar. Ecol. Prog. Ser. **60:** 113–122.

———, O. SCHOFIELD, AND B. B. PRÉZELIN. 1989. Influence of zeaxanthin on quantum yield of photosynthesis of *Synechococcus* clone WH7803 (DC2). Mar. Ecol. Prog. Ser. **56:** 177–188.

BIENFANG, P. K., AND J. P. SZYPER. 1981. Phytoplankton dynamics in the subtropical Pacific off Hawaii. Deep-Sea Res. **28:** 981–1000.

———, ———, M. Y. OKAMOTO, AND E. K. NODA. 1984. Temporal and spatial variability of phytoplankton in a subtropical ecosystem. Limnol. Oceanogr. **29:** 527–539.

CARPENTER, E. J., AND K. ROMANS. 1991. Major role of the cyanobacterium *Trichodesmium* in nutrient cycling in the North Atlantic Ocean. Science **254:** 1356–1358.

CHISWELL, S., E. FIRING, D. KARL, R. LUKAS, AND C. WINN. 1990. Hawaii Ocean Time-series data report 1. Univ. Hawaii, SOEST Tech. Rep. 90-1.

CUSHING, D. H. 1959. The seasonal variation in oceanic production as a problem in population dynamics. J. Cons. Cons. Int. Explor. Mer **24:** 455–464.

DEVASSY, V. P., P. M. A. BHATTATHIRI, AND S. Z. QUASIM. 1978. *Trichodesmium* phenomenon. Indian J. Mar. Sci. **7:** 168–186.

———, ———, AND ———. 1979. Succession of organisms following *Trichodesmium* phenomenon. Indian J. Mar. Sci. **8:** 89–93.

DITULLIO, G. R., AND E. A. LAWS. 1991. Impact of an atmospheric-oceanic disturbance on phytoplankton community dynamics in the North Pacific central gyre. Deep-Sea Res. **38:** 1305–1329.

DONAGHAY, P. L., AND OTHERS. 1991. The role of episodic atmospheric nutrient inputs in the chemical and biological dynamics of oceanic ecosystems. Oceanography **4:** 62–70.

EPPLEY, R. W., E. H. RENGER, E. L. VENRICK, AND M. M. MULLIN. 1973. A study of phytoplankton dynamics and nutrient cycling in the central gyre of the North Pacific Ocean. Limnol. Oceanogr. **18:** 534–551.

FALKOWSKI, P. G., D. ZIEMANN, Z. KOLBEA, AND P. I. BIENFANG. 1991. Role of eddy pumping in enhancing primary production in the ocean. Nature **352:** 55–58.

GIESKES, W. W., AND G. W. KRAAY. 1986. Floristic and physiological differences between the shallow and the deep nanophytoplankton community in the euphotic zone of the open tropical Atlantic revealed by HPLC analysis of pigments. Mar. Biol. **91:** 567–576.

GOERICKE, R., AND D. J. REPETA. 1992. The pigments of *Prochlorococcus marinus*: The presence of divinyl chlorophyll *a* and *b* in a marine procaryote. Limnol. Oceanogr. **37:** 425–433.

HAYWARD, T. L. 1987. The nutrient distribution and primary production in the central North Pacific. Deep-Sea Res. **34:** 1593–1627.

———, AND J. A. MCGOWAN. 1985. Spatial patterns of chlorophyll, primary production, macrozooplankton biomass, and physical structure in the central North Pacific Ocean. J. Plankton Res. **7:** 147–167.

———, AND E. L. VENRICK. 1982. Relation between surface chlorophyll and integrated production. Mar. Biol. **69:** 247–252.

———, ———, AND J. A. MCGOWAN. 1983. Environmental heterogeneity and plankton community in the central North Pacific. J. Plankton Res. **41:** 711–729.

HEINRICH, A. K. 1962. The life history of plankton animals and seasonal cycles of plankton communities in the oceans. J. Cons. Cons. Int. Explor. Mer **27:** 15–24.

KANA, T. M., P. M. GLIBERT, R. GOERICKE, AND N. A. WELSCHMEYER. 1988. Zeaxanthin and β-carotene in *Synechococcus* WH7803. Limnol. Oceanogr. **33:** 1623–1627.

KARL, D. M. 1980. Cellular nucleotide measurements and applications in microbial ecology. Microbiol. Rev. **44:** 739–796.

———, R. LETELIER, D. V. HEBEL, D. F. BIRD, AND C. WINN. 1992. *Trichodesmium* blooms and new nitrogen in the North Pacific gyre, p. 219–237. *In* E. J. Carpenter et al. [eds.], Marine pelagic cyanobacteria: *Trichodesmium* and other diazotrophs. Kluwer.

———, AND C. D. WINN. 1991. A sea of change: Monitoring the oceans' carbon cycle. Environ. Sci. Technol. **25:** 1976–1981.

KIRK, J. T. O. 1983. Light and photosynthesis in aquatic ecosystems. Cambridge.

LAWS, E. A., D. M. KARL, D. G. REDALJE, R. S. JURICK, AND C. D. WINN. 1983. Variability in ratios of phytoplankton carbon and RNA to ATP and chlorophyll *a* in batch and continuous cultures. J. Phycol. **19:** 439–445.

———, AND OTHERS. 1984. High phytoplankton growth and production rates in oligotrophic Hawaiian coastal waters. Limnol. Oceanogr. **29:** 1161–1169.

MCGOWAN, J. A., AND T. L. HAYWARD. 1978. Mixing and oceanic productivity. Deep-Sea Res. **25:** 771–793.

MARTIN, J. H. 1991. Iron, Liebig's law, and the greenhouse. Oceanography **4:** 52–55.

OHMAN, M. D. G., G. C. ANDERSON, AND E. OZTURGUT. 1982. A multivariable analysis of planktonic interactions in the eastern tropical North Pacific. Deep-Sea Res. **29:** 1451–1469.

ONDRUSEK, M. E., R. R. BIDIGARE, S. T. SWEET, D. A. DEFREITAS, AND J. M. BROOKS. 1991. Distributions of phytoplankton pigments in the North Pacific Ocean in relation to physical and optical variability. Deep-Sea Res. **38:** 243–266.

PARTENSKY, F., N. HOEPFFNER, W. K. W. LI, O. ULLOA, AND D. VAULOT. 1993. Photoacclimation of *Prochlorococcus* sp. (Prochlorophyta) strains isolated from the North Atlantic and the Mediterranean Sea. Plant Physiol. **101:** 285–296.

PLATT, T., AND W. G. HARRISON. 1985. Biogenic fluxes of carbon and oxygen in the ocean. Nature **318:** 55–58.

SHUTER, B. 1979. A model of physiological adaptation in unicellular algae. J. Theor. Biol. **78:** 519–552.

SOURNIA, A. 1969. Cycle annuel du phytoplancton et de la production primaire dans les mers tropicales. Mar. Biol. **3:** 287–303.

STAUBER, J. L., AND S. W. JEFFREY. 1988. Photosynthetic pigments in 51 species of marine diatoms. J. Phycol. **24:** 158–172.

TANGEN, K., AND T. BJÖRNLAND. 1981. Observations on pigments and morphology of *Gyrodinium aureolum* Hulburt, a marine dinoflagellate containing 19'-hexanoyloxyfucoxanthin as the main carotenoid. J. Plankton Res. **3:** 389–401.

TARANTOLA, A. 1987. Inverse problem theory: Methods for data fitting and parameter estimation, 1st ed. Elsevier.

THOMAS, W. H. 1970. On nitrogen deficiency in tropical Pacific Ocean phytoplankton: Photosynthetic parameters in poor and rich water. Limnol. Oceanogr. **15:** 380–385.

TRIOLA, M. 1989. Elementary statistics, 4th ed. Cummings.

VENRICK, E. L. 1979. The lateral extent and characteristics of the North Pacific central environment at 35°N. Deep-Sea Res. **26:** 1153–1178.

———. 1990. Mesoscale patterns of chlorophyll *a* in the central North Pacific. Deep-Sea Res. **37:** 1017–1031.

———, J. A. MCGOWAN, D. R. CAYAN, AND T. L. HAYWARD. 1987. Climate and chlorophyll *a*: Long-term trends in the central North Pacific Ocean. Science **238:** 70–72.

VESK, M., AND S. W. JEFFREY. 1987. Ultrastructure and pigments of two strains of the picoplanktonic alga *Pelagococcus subviridis* (Chrysophyceae). J. Phycol. **23:** 322–336.

WINN, C., S. CHISWELL, E. FIRING, D. KARL, AND R. LUKAS. 1991. Hawaii Ocean Time-series data report 2. Univ. Hawaii, SOEST Tech. Rep. 92-1.

———, R. LUKAS, D. KARL, AND E. FIRING. 1993. Hawaii Ocean Time-series data report 3. Univ. Hawaii, SOEST Tech. Rep. 93-3.

WITHERS, N. W., A. FIKSDAHL, R. C. TUTTLE, AND S. LIAEEN-JENSEN. 1981. Carotenoids of the chrysophyceae. Comp. Biochem. Physiol. **68B:** 345–349.

YOUNG, R. W., AND OTHERS. 1991. Atmospheric iron inputs and primary productivity: Phytoplankton responses in the North Pacific. Global Biogeochem. Cycles **5:** 119–134.

Submitted: 20 May 1992
Accepted: 26 February 1993
Revised: 7 May 1993